
EPSILON-GREEDY THOMPSON SAMPLING TO BAYESIAN OPTIMIZATION

A PREPRINT

Bach Do

Department of Civil and Environmental Engineering
University of Houston
Houston, TX 77004
bdo3@uh.edu

Ruda Zhang

Department of Civil and Environmental Engineering
University of Houston
Houston, TX 77004
rudaz@uh.edu

ABSTRACT

Thompson sampling (TS) serves as a solution for addressing the exploitation-exploration dilemma in Bayesian optimization (BO). While it prioritizes exploration by randomly generating and maximizing sample paths of Gaussian process (GP) posteriors, TS weakly manages its exploitation by gathering information about the true objective function after each exploration is performed. In this study, we incorporate the epsilon-greedy (ε -greedy) policy, a well-established selection strategy in reinforcement learning, into TS to improve its exploitation. We first delineate two extremes of TS applied for BO, namely the generic TS and a sample-average TS. The former and latter promote exploration and exploitation, respectively. We then use ε -greedy policy to randomly switch between the two extremes. A small value of $\varepsilon \in (0, 1)$ prioritizes exploitation, and vice versa. We empirically show that ε -greedy TS with an appropriate ε is better than one of its two extremes and competes with the other.

Keywords Thompson sampling · Epsilon-greedy policy · Bayesian optimization

1 Introduction

We consider the following minimization problem:

$$\begin{aligned} \min_{\mathbf{x}} \quad & f(\mathbf{x}) \\ \text{s.t.} \quad & \mathbf{x} \in \mathcal{X}, \end{aligned} \tag{1}$$

where $\mathbf{x} \in \mathbb{R}^d$ is the vector of d input variables selected in a bounded, compact domain \mathcal{X} , and $f : \mathbb{R}^d \mapsto \mathbb{R}$ is a real-valued objective function. In science and engineering, $f(\mathbf{x})$ is often costly to compute which unfortunately hinders the use of any standard derivative-based optimizers.

Bayesian optimization (BO) is a global optimization technique that relies on a probabilistic model of the objective function, coupled with an optimization policy to guide the optimization process [1–4]. BO demonstrates its remarkable performance when optimizing small- to moderate-dimensional optimization problems with costly or black-box objective functions. Given a dataset consisting of several observations of the input variables and the objective function, a Gaussian process (GP) posterior built from this dataset often serves as the probabilistic model representing our beliefs about the objective function. Meanwhile, the optimization policy specifying what we value in the dataset is defined through an acquisition function. This acquisition function is cost-effective to evaluate given the GP posterior, making it convenient for processing optimization. Different considerations to derive the optimization policy include (1) the value of the objective function [5], (2) the information about the minimum location [6–8], and (3) the information about the minimum value [9]. Several notable acquisition functions, including expected improvement (EI) [10], weighted EI [11], GP upper confidence bound (GP-UCB) [12], and knowledge gradient [13], are developed to balance exploitation and exploration.

Thompson sampling (TS) is a stochastic policy to address the exploitation-exploration dilemma in multi-armed bandit problems [14, 15]. In each iteration, TS selects an arm from a set of finite arms. Each arm corresponds to a stochastic

reward from an unknown distribution. The goal is to craft a sequence of arms that maximizes the cumulative reward under assumption that the rewards are independent of time and conditionally independent given the selected arms.

When applied to BO, (the generic) TS generates a sequence of input variable points through a mechanism that involves random sampling from an unknown posterior distribution of the global minimum location [16]. Thus, we can consider TS a BO method of a random acquisition function. Several information-theoretic optimization policies also compute their acquisition functions based on a set of samples generated by TS [8, 9]. When the GP posterior exhibits high uncertainty, TS tends to produce diverse input variable points during the optimization process, thereby prioritizing exploration. As the number of observations increases, it transitions to exploiting the knowledge gained about the true objective function. Such an exploitation strategy, however, is inferior due to the randomness of TS. This motivates the quest for an intervention to improve the exploitation of TS.

In this work, we incorporate ε -greedy policy into TS to improve its exploitation. ε -greedy policy is a selection strategy in reinforcement learning to address the exploitation-exploration dilemma [17]. Given $\varepsilon \in (0, 1)$, the policy chooses an action by either maximizing the average reward function with probability $1 - \varepsilon$ or selecting it randomly with probability ε . The selection strategy is pure exploitation (i.e., greedy) when $\varepsilon = 0$, or pure exploration when $\varepsilon = 1$. Our approach performs the generic TS (with probability ε) for exploration and a new fashion of TS called sample-average TS (with probability $1 - \varepsilon$) for exploitation.

Several works have introduced ε -greedy policy to BO and multi-armed bandit problems. De Ath et al. [18] proposed two schemes for applying the policy to BO. The first scheme performs exploration (with probability ε) by randomly selecting a point on the Pareto frontier that is obtained by minimizing the posterior mean and maximizing the posterior standard deviation simultaneously. The second scheme performs exploration by randomly selecting a point in the input variable space. Both schemes implement exploitation (with probability $1 - \varepsilon$) by minimizing the posterior mean function. Jin et al. [19] introduced the so-called ε -exploring TS to multi-armed bandit problems. Given the posterior distributions of aims, exploration (with probability ε) sets the estimated reward function for each aim as a random sample drawn from the associated posterior distribution, while exploitation (with probability $1 - \varepsilon$) sets the estimated reward function as the sample mean function. However, the performance of ε -greedy TS for BO is still unexplored.

Our contributions are as follows: (1) ε -greedy TS to BO, which is a simple, computation-efficient method to improve the exploitation of TS; and (2) empirical evaluations demonstrating that ε -greedy TS with appropriate ε is better than one of its two extremes (i.e., the generic TS and the sample-average TS) and competes with the other.

Section 2 provides a general background needed to develop ε -greedy TS. Section 3 describes the method. The experimental evaluation and discussion are given in Section 4.

2 Background

2.1 Gaussian processes

Consider a training dataset $\mathcal{D} = \{\mathbf{X}, \mathbf{Y}\} = \{\mathbf{x}^k, y^k\}_{k=1}^N$, where $\mathbf{x}^k \in \mathbb{R}^d$ are observations of d -dimensional vectors of input variables, and $y^k \in \mathbb{R}$ denote the corresponding observations of the objective function. We wish to build from \mathcal{D} a mapping $y(\mathbf{x}) = f(\mathbf{x}) + \varepsilon_n : \mathbb{R}^d \mapsto \mathbb{R}$, where $f(\mathbf{x})$ is a regression function and $\varepsilon_n \sim \mathcal{N}(0, \sigma_n^2)$ is an additive zero-mean Gaussian noise with variance σ_n^2 . This observation noise is assumed to be independent and identically distributed.

A GP assumes that any finite subset of an infinite set of regression function values has a joint Gaussian distribution [20]. This is encoded in the following GP prior:

$$f(\cdot) \sim \mathcal{GP}(0, \kappa(\cdot, \cdot | \boldsymbol{\theta}_x)), \quad (2)$$

where $\kappa(\mathbf{x}, \mathbf{x}' | \boldsymbol{\theta}_x) = \text{cov}[f(\mathbf{x}), f(\mathbf{x}')] : \mathbb{R}^d \times \mathbb{R}^d \mapsto \mathbb{R}$ is a positive semi-definite covariance function parameterized by a vector $\boldsymbol{\theta}_x$ of hyperparameters.

By conditioning such prior knowledge on \mathcal{D} and utilizing the observation noise assumption, we can show that the vector of observations $\{y(\mathbf{x}^1), \dots, y(\mathbf{x}^N)\}$ is distributed according to an N -variate Gaussian with zero mean and covariance matrix $\mathbf{A} = \mathbf{K} + \sigma_n^2 \mathbf{I}_N$, where the (i, j) th element of \mathbf{K} is $\kappa(\mathbf{x}^i, \mathbf{x}^j | \boldsymbol{\theta}_x)$ and \mathbf{I}_N denotes an N -by- N identity matrix. By further applying the conditional multivariate Gaussian [21], we obtain the posterior predictive distribution at an unseen input variable vector \mathbf{x}^* , i.e., $p(f(\mathbf{x}^*) | \mathbf{x}^*, \mathcal{D}) = \mathcal{N}(\mu_f(\mathbf{x}^*), \sigma_f^2(\mathbf{x}^*))$, which contains the information about the mapping we wish to build. The predictive mean and variance are

$$\mu_f(\mathbf{x}^*) = \mathbf{K}^{*\top} \mathbf{A}^{-1} \mathbf{Y}, \quad (3)$$

$$\sigma_f^2(\mathbf{x}^*) = \kappa(\mathbf{x}^*, \mathbf{x}^* | \boldsymbol{\theta}_x) - \mathbf{K}^{*\top} \mathbf{A}^{-1} \mathbf{K}^*, \quad (4)$$

where

$$\mathbf{K}^* = [\kappa(\mathbf{x}^*, \mathbf{x}^1 | \boldsymbol{\theta}_x), \dots, \kappa(\mathbf{x}^*, \mathbf{x}^N | \boldsymbol{\theta}_x)]^\top. \quad (5)$$

Algorithm 1 Generic Thompson sampling for Bayesian optimization.

```

1: input: input variable domain  $\mathcal{X}$ , number of initial observations  $N$ , threshold for number of BO iterations  $K$ 
2: Generate  $N$  samples of  $\mathbf{x}$  using Latin hypercube sampling
3: for  $i = 1 : N$  do
4:    $y^i \leftarrow f(\mathbf{x}^i) + \varepsilon_n^i$ 
5: end for
6:  $\mathcal{D}^0 \leftarrow \{\mathbf{x}^i, y^i\}_{i=1}^N$ 
7:  $\{\mathbf{x}_{\min}, y_{\min}\} \leftarrow \min\{y^i, i = 1, \dots, N\}$ 
8: for  $k = 1 : K$  do
9:   Build a GP posterior  $\hat{f}^k(\mathbf{x})|\mathcal{D}^{k-1}$ 
10:  Generate a sample path  $g(\mathbf{x}|\mathcal{D}^{k-1})$  from  $\hat{f}^k(\mathbf{x})|\mathcal{D}^{k-1}$ 
11:   $\mathbf{x}^k \leftarrow \arg \min_{\mathbf{x}} g(\mathbf{x}|\mathcal{D}^{k-1})$  s.t.  $\mathbf{x} \in \mathcal{X}; \mathbf{x} \notin \mathcal{D}^{k-1}$ 
12:   $y^k \leftarrow f(\mathbf{x}^k) + \varepsilon_n^k$ 
13:   $\mathcal{D}^k \leftarrow \mathcal{D}^{k-1} \cup \{\mathbf{x}^k, y^k\}$ 
14:   $\{\mathbf{x}_{\min}, y_{\min}\} \leftarrow \min\{y_{\min}, y^k\}$ 
15: end for
16: return  $\{\mathbf{x}_{\min}, y_{\min}\}$ 

```

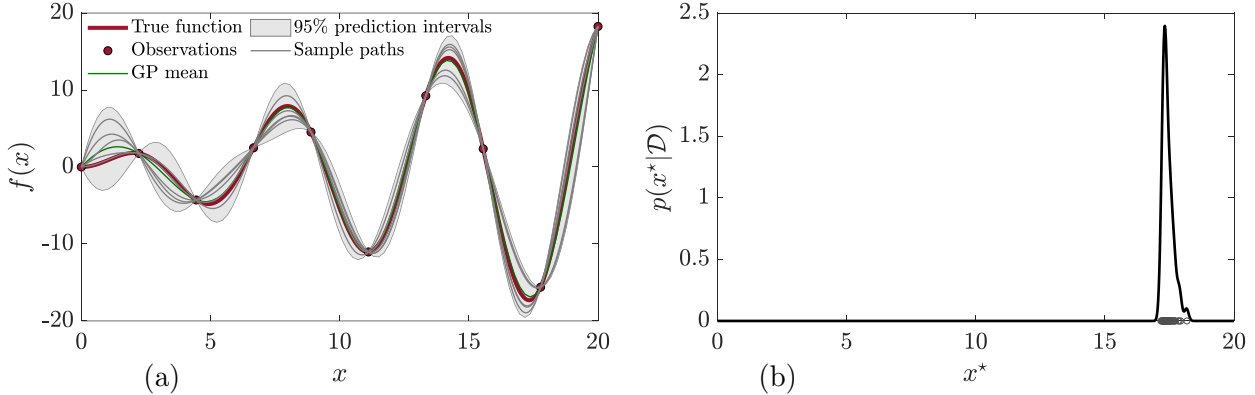


Figure 1: Sample paths from the GP posterior for $f(x) = x \sin(x)$ and distribution of their minimums. (a) GP predictions and five sample paths drawn from the GP posterior; and (b) Approximate distribution of $p(x^*|\mathcal{D})$ obtained from minimizing 50 sample paths.

2.2 Bayesian optimization via Thompson sampling

As described in Section 1, the generic TS generates a sequence of input variable points \mathbf{x}^k ($k = 1, \dots, K$) using a mechanism that involves random sampling from an unknown posterior distribution $p(\mathbf{x}^*|\mathcal{D}_{k-1})$ of the global minimum \mathbf{x}^* . Here K represents a finite budget on the number of BO iterations. Leveraging the fact that \mathbf{x}^* is fully determined by the objective function, the generic TS follows two simple steps in each iteration. First, it draws a sample path from the GP posterior $\hat{f}^k(\mathbf{x})|\mathcal{D}^{k-1}$ for which the detailed implementation is given in Section 2.3. It then minimizes the obtained sample path to find a sample \mathbf{x}^* that is assigned as the new input point \mathbf{x}^k . Algorithm 1 summarizes the implementation of the generic TS.

Figure 1 shows several sample paths generated from the GP posterior of function $f(x) = x \sin x$ and an approximate distribution of their minimum locations. More specifically, a GP model with zero mean and squared exponential covariance function is first built from ten observations. A total of 50 sample paths are then drawn, and five of them are shown in Figure 1(a). Minimizing the generated sample paths and using a kernel density estimation for the obtained solutions result in an approximate distribution of $p(\mathbf{x}^*|\mathcal{D})$ as shown in Figure 1(b). Note that the generic TS in Algorithm 1 generates only one sample path in each iteration and does not attempt to approximate the posterior distribution of the minimum location.

Algorithm 2 Generation of sample paths using random features.

- 1: **Input:** dataset \mathcal{D}_{k-1} , type of stationary covariance function $\kappa(\cdot, \cdot | \theta_x)$, number of spectral points N_p
- 2: Build a GP model from \mathcal{D}_{k-1}
- 3: Derive $p(\mathbf{s})$ from the posterior covariance function $\kappa(\cdot, \cdot | \theta_x)$
- 4: **for** $i = 1 : N_p$ **do**
- 5: $[\mathbf{W}]_i \sim p(\mathbf{s})$
- 6: $[\mathbf{b}]_i \sim \mathcal{U}[0, 2\pi]$
- 7: **end for**
- 8: Formulate $\phi(\mathbf{x})$; see Equation (7)
- 9: $\Phi \leftarrow [\phi(\mathbf{x}), \dots, \phi(\mathbf{x}^N)]$
- 10: Compute μ_β and Σ_β ; see Equation (9)
- 11: $\beta \sim \mathcal{N}(\mu_\beta, \Sigma_\beta)$
- 12: **return** $g(\mathbf{x}) | \mathcal{D}^{k-1} \leftarrow \beta^\top \phi(\mathbf{x})$

2.3 Sampling from Gaussian process posteriors

Given the GP posterior $\hat{f}^k(\mathbf{x}) | \mathcal{D}^{k-1}$ characterized by a stationary covariance function, we follow the spectral sampling approach by Hernández-Lobato et al. [8] to generate a sample path $g(\mathbf{x} | \mathcal{D}^{k-1})$ in Line 10 of Algorithm 1. This approach approximates the GP prior in Equation (2) using a Bayesian linear model of randomized feature maps. Such an approximation is rooted in Bochner's theorem that guarantees the existence of a Fourier dual $p(\mathbf{s})$ ($\mathbf{s} \in \mathbb{R}^d$) of the stationary covariance function, which is called spectral density when a finite non-negative Borel measure is interpreted as a distribution [22]. The spectral density functions corresponding to several isotropic covariance functions of Matérn class can be found in Riutort-Mayol et al. [23]. Once $p(\mathbf{s})$ is determined, we can represent $\kappa(\mathbf{x}, \mathbf{x}' | \theta_x)$ by the following randomized feature map [24]:

$$\kappa(\mathbf{x}, \mathbf{x}' | \theta_x) = \phi(\mathbf{x})^\top \phi(\mathbf{x}'). \quad (6)$$

The the feature map $\phi(\mathbf{x})$ can be approximated by [8]

$$\phi(\mathbf{x}) = \sqrt{2\kappa(0 | \theta_x) / N_p} \cos(\mathbf{W}\mathbf{x}^\top + \mathbf{b}), \quad (7)$$

where \mathbf{W} and \mathbf{b} stack N_p spectral points generated from $p(\mathbf{s})$ and N_p points drawn from the uniform distribution $\mathcal{U}[0, 2\pi]$, respectively; and $\kappa(0 | \theta_x)$ is well defined because $\kappa(\mathbf{x}, \mathbf{x}' | \theta_x)$ is a stationary covariance function, which reads $\kappa(\mathbf{x}, \mathbf{x}' | \theta_x) = \kappa(\|\mathbf{x} - \mathbf{x}'\| | \theta_x)$.

Once the approximate feature map is formulated, the GP prior as a kernel machine can be approximated by the following Bayesian linear model:

$$f(\mathbf{x}) \approx \beta^\top \phi(\mathbf{x}), \quad (8)$$

where the weight vector β is a multivariate Gaussian. By conditioning Equation (8) on the data, we obtain the mean and covariance matrix of conditional β , as

$$\mu_\beta = (\Phi^\top \Phi + \sigma_n^2 \mathbf{I}_N)^{-1} \Phi^\top \mathbf{y}, \quad (9a)$$

$$\Sigma_\beta = (\Phi^\top \Phi + \sigma_n^2 \mathbf{I}_N)^{-1} \sigma_n^2, \quad (9b)$$

where $\Phi = [\phi(\mathbf{x}), \dots, \phi(\mathbf{x}^N)] \in \mathbb{R}^{N_p \times N}$.

In summary, the generation of $g(\mathbf{x} | \mathcal{D}^{k-1})$ using random features is detailed in Algorithm 2. Note that Line 10 of Algorithm 2 involves the Cholesky decomposition of matrix $(\Phi^\top \Phi + \sigma_n^2 \mathbf{I}_N)$ to facilitate the calculation of its inverse. To increase the accuracy of sample paths, we may use alternative posterior sampling techniques such as the decoupled sampling method [25].

3 Epsilon-greedy Thompson sampling to Bayesian optimization

3.1 Thompson sampling via sample-average method

In addition to the generic TS, we perform another form of TS for BO via the sample-average method [26]. This technique, referred to as sample-average TS (or simply averaging TS), is to enhance the exploitation of TS. More

Algorithm 3 ε -greedy Thompson sampling for Bayesian optimization.

```

1: input: input variable domain  $\mathcal{X}$ , number of initial observations  $N$ , threshold for number of BO iterations  $K$ ,  

   number of spectral points  $N_p$ , number of sample paths  $N_s$ , value of  $\varepsilon \in (0, 1)$ 
2: Generate  $N$  samples of  $\mathbf{x}$ 
3: for  $i = 1 : N$  do
4:    $y^i \leftarrow f(\mathbf{x}^i) + \varepsilon_n^i$ 
5: end for
6:  $\mathcal{D}^0 \leftarrow \{\mathbf{x}^i, y^i\}_{i=1}^N$ 
7:  $\{\mathbf{x}_{\min}, y_{\min}\} \leftarrow \min\{y^i, i = 1, \dots, N\}$ 
8: for  $k = 1 : K$  do
9:   Build a GP posterior  $\hat{f}^k(\mathbf{x})|\mathcal{D}^{k-1}$ 
10:  Generate  $r \sim \mathcal{U}[0, 1]$ 
11:  if  $r \leq \varepsilon$  then
12:    Generate  $g(\mathbf{x}|\mathcal{D}^{k-1})$  from  $\hat{f}^k(\mathbf{x})|\mathcal{D}^{k-1}$ 
13:  else
14:    for  $s = 1 : N_s$  do
15:      Generate  $h^s(\mathbf{x}|\mathcal{D}^{k-1})$  from  $\hat{f}^k(\mathbf{x})|\mathcal{D}^{k-1}$ 
16:    end for
17:     $g(\mathbf{x}|\mathcal{D}^{k-1}) \leftarrow \frac{1}{N_s} \sum_{s=1}^{N_s} h^s(\mathbf{x}|\mathcal{D}^{k-1})$ 
18:  end if
19:   $\mathbf{x}^k \leftarrow \arg \min_{\mathbf{x}} g(\mathbf{x}|\mathcal{D}^{k-1})$  s.t.  $\mathbf{x} \in \mathcal{X}; \mathbf{x} \notin \mathcal{D}^{k-1}$ 
20:   $y^k \leftarrow f(\mathbf{x}^k) + \varepsilon_n^k$ 
21:   $\mathcal{D}^k \leftarrow \mathcal{D}^{k-1} \cup \{\mathbf{x}^k, y^k\}$ 
22:   $\{\mathbf{x}_{\min}, y_{\min}\} \leftarrow \min\{y_{\min}, y^k\}$ 
23: end for
24: return  $\{\mathbf{x}_{\min}, y_{\min}\}$ 

```

specifically, we call Algorithm 2 to generate in Line 10 of Algorithm 1 a total of N_s sample paths $h^s(\mathbf{x}|\mathcal{D}^{k-1})$ ($s = 1, \dots, N_s$). These sample paths are then used to define the following average sample path:

$$g(\mathbf{x}|\mathcal{D}^{k-1}) = \frac{1}{N_s} \sum_{s=1}^{N_s} h^s(\mathbf{x}|\mathcal{D}^{k-1}). \quad (10)$$

Finally, we minimize $g(\mathbf{x}|\mathcal{D}^{k-1})$ to find the new input variable point. This approach differs from that of Balandat et al. [26] which generates the sample paths using randomized quasi Monte-Carlo techniques.

We see that if $N_s = \infty$, $g(\mathbf{x}|\mathcal{D}^{k-1})$ in Equation (10) is indeed the GP posterior mean in Equation (3) whose minimum tends to promote exploitation. If $N_s = 1$, the sample-average TS recovers the generic TS that favors exploration. Between these extremes, therefore, is an unknown value of N_s at which TS balances exploitation and exploration. However, we do not attempt to find such a value in this work. We instead set N_s at a sufficiently large value, say $N_s = 50$.

3.2 ε -greedy Thompson sampling

We see that the generic TS and the averaging TS for a sufficiently large number of sample paths represent two extremes of TS: the former and latter address exploration and exploitation, respectively. This distinction motivates our approach that uses ε -greedy policy to randomly switch between these extremes. Accordingly, we implement the generic TS with probability ε to explore the input variable space. We implement the averaging TS with probability $1 - \varepsilon$ to guide the search toward exploitation. We do not use the posterior mean in Equation (3) for exploitation because we observe that computing its derivatives is more expensive than computing the derivatives of the average sample path in Equation (10). Moreover, it is straightforward to recover the generic TS by simply setting $\varepsilon = 1$ or $N_s = 1$. Algorithm 3 details the ε -greedy TS when applied to BO.

Our approach addresses the exploitation-exploration dilemma by the following factors: (1) ε – a small ε promotes exploitation, and vice versa; (2) N_s – a sufficiently large N_s encourages exploitation; and (3) the accuracy of GP model – an accurate GP model can induce significant exploitation.

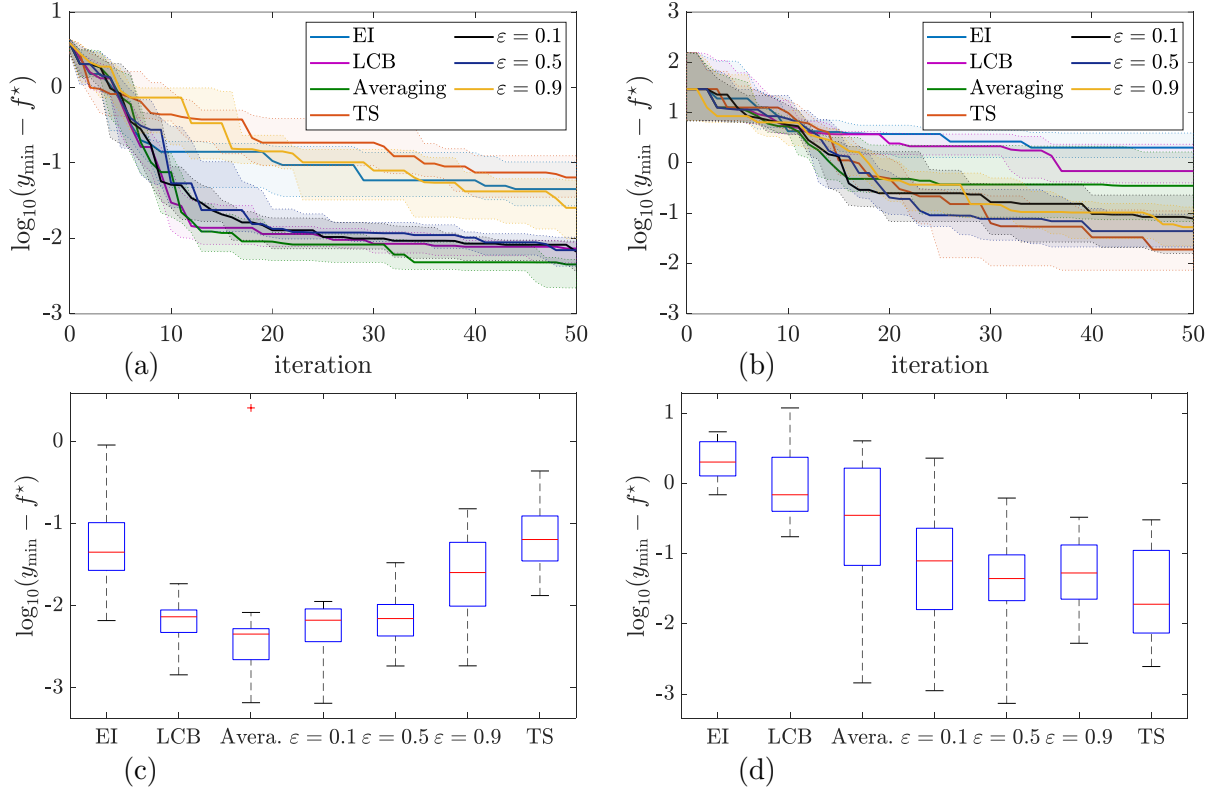


Figure 2: Performance of EI, LCB, averaging TS, generic TS, and ε -greedy TS methods for 2d Ackley and 2d Rosenbrock functions. Medians and interquartile ranges from 15 runs of each method for (a) 2d Ackley function and (b) 2d Rosenbrock function; Medians, and the 25th and 75th percentiles from 15 best-found observations at iteration 50 for (c) 2d Ackley function and (d) 2d Rosenbrock function.

4 Experiments

We test the empirical performance of ε -greedy TS on challenging optimization problems of four benchmark functions: the 2d Akley function, the 2d Rosenbrock function, the 6d Hartmann function, and the 10d Michalewicz function. The analytical expressions for these functions and their global minimums are given in Appendix A. In our experiments, we use the squared exponential covariance function for building GP models. To find optimal hyperparameters for each problem, we follow Bradford et al. [27] and use the DIRECT algorithm [28] whose output is then set as the initial point of a derivative-based optimizer. We carry out all experiments using a PC with an Intel Core i7-1165G7 2.80 GHz CPU and 8.0 GB memory. We compare the optimization results from ε -greedy TS with those from other BO methods, including EI, the lower confidence bound (LCB), the averaging TS, and the generic TS.

We randomly generate 15 initial datasets for each problem using Latin hypercube sampling [29]. We then start each BO method from each of these datasets. In each optimization iteration, we record the best-found observation value of the observation error $\log_{10}(y_{\min} - f^*)$ and the corresponding input variable vector. Here y_{\min} and f^* represent the best observation of the objective function found in each iteration and its true minimum value, respectively. For the 2d Akley and 2d Rosenbrock functions, we set the number of initial observations and the number of BO iterations at $N = 10d$ and $K = 50$. For the 6d Hartmann and 10d Michalewicz functions, we set $N = 5d$ and $K = 100$. In all experiments, we sample 1000 spectral points to formulate each sample path.

4.1 Optimization results

Figure 2 shows the medians and interquartile ranges from 15 runs of each BO method for the 2d Akley and 2d Rosenbrock functions. Figure 3 shows similar quantities for the 6d Hartmann and 10d Michalewicz functions. In general, the optimization results from ε -greedy TS for an appropriate ε are better than those from one of its two extremes (i.e., averaging and the generic TS) and competitive with the results from the other. However, differences in performances of these methods are minor for the 6d Hartmann and 10d Michalewicz functions. This may be attributed

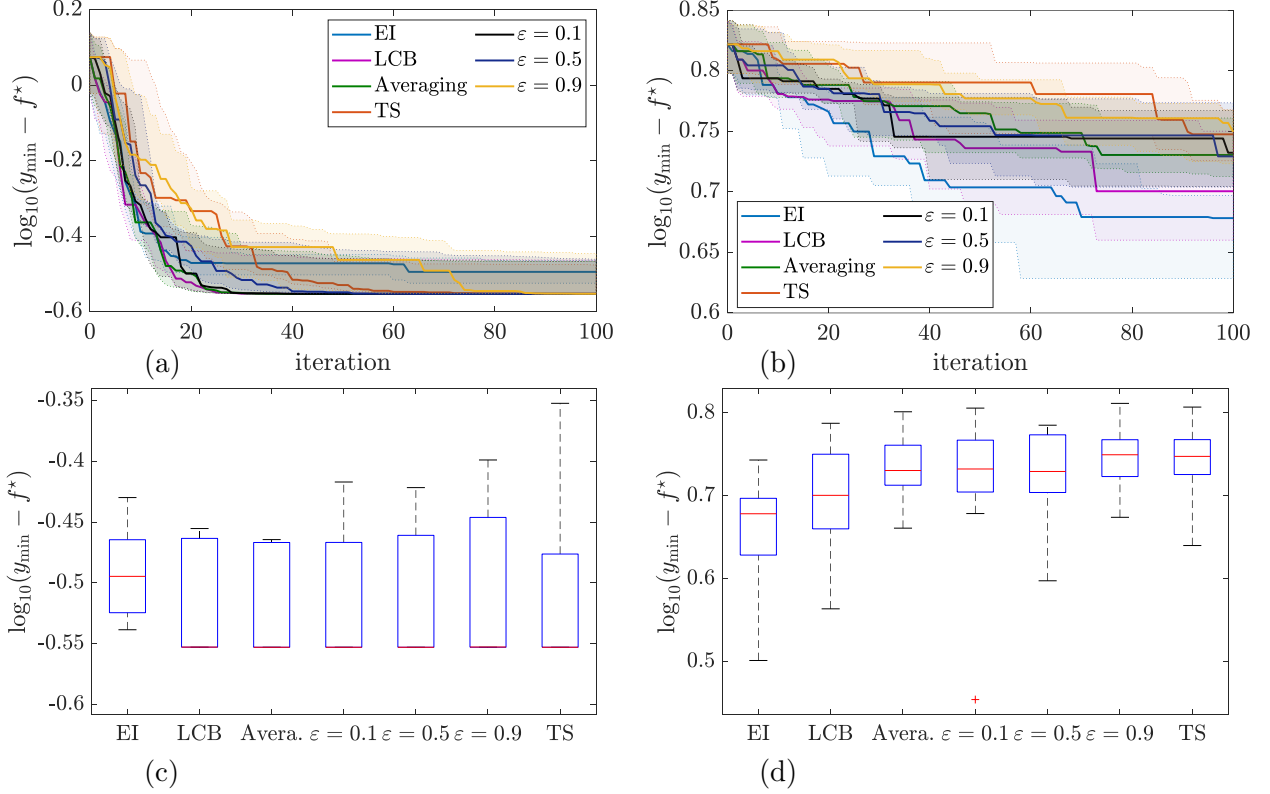


Figure 3: Performance of EI, LCB, averaging TS, generic TS, and ε -greedy TS methods for 6d Hartmann and 10d Michalewicz functions. Medians and interquartile ranges from 15 runs of each method for (a) 6d Hartmann function and (b) 10d Michalewicz function; Medians, and the 25th and 75th percentiles from 15 best-found observations at iteration 100 for (c) 6d Hartmann function and (d) 10d Michalewicz function.

to exploration arising from the inaccuracy of GP models in high-dimensional spaces. In other words, deliberate exploitation of ε -greedy TS is hindered by an increase in the number of input variables. With a proper ε value, ε -greedy TS can provide the best objective values among those from the considered TS methods. The advantage of ε -greedy TS over EI or LCB is problem-dependent.

4.2 Effect of ε values

We investigate the effects of ε values on the performance of ε -greedy TS. For the 2d Akley and 2d Rosenbrock functions, we set $\varepsilon \in \{0.1, 0.3, 0.5, 0.7, 0.9\}$ and fix N_s at 50. We use $\varepsilon \in \{0.1, 0.5, 0.9\}$ and $N_s = 50$ for the 6d Hartmann and 10d Michalewicz functions.

As shown in Figures 3(c) and 4(c), the performance of ε -greedy TS for the 2d Akley and 6d Hartmann functions becomes worse when using a large value of ε . The method works well for a moderate value of ε when minimizing the 2d Rosenbrock and 10d Michalewicz functions; see Figures 3(d) and 4(d). The observed trends of optimization results when varying ε suggest that there exists an optimal ε that corresponds to the best performance of ε -greedy TS for each problem. Such an optimal value, for example, may be selected from $[0.1, 0.5]$ for the 2d Akley function, or from $[0.3, 0.7]$ for the 2d Rosenbrock function; see Figures 4(c) and (d).

As discussed in Section 1, increasing ε results in more exploration of an ε -greedy strategy. For ε -greedy TS, increasing ε encourages the algorithm to explore more unseen regions of input variable space, which is confirmed in Figures 8 and 9 of Appendix B.

4.3 On selection of optimal ε

While our optimization results indicate that it is safe to set $\varepsilon = 0.5$ to balance exploitation and exploration, an optimal ε strongly depends on the problem of interest. A problem that requires more exploration to find an optimal solution (e.g., the 2d Rosenbrock function) may benefit from a large ε value. Meanwhile, a problem requiring more exploitation (e.g.,

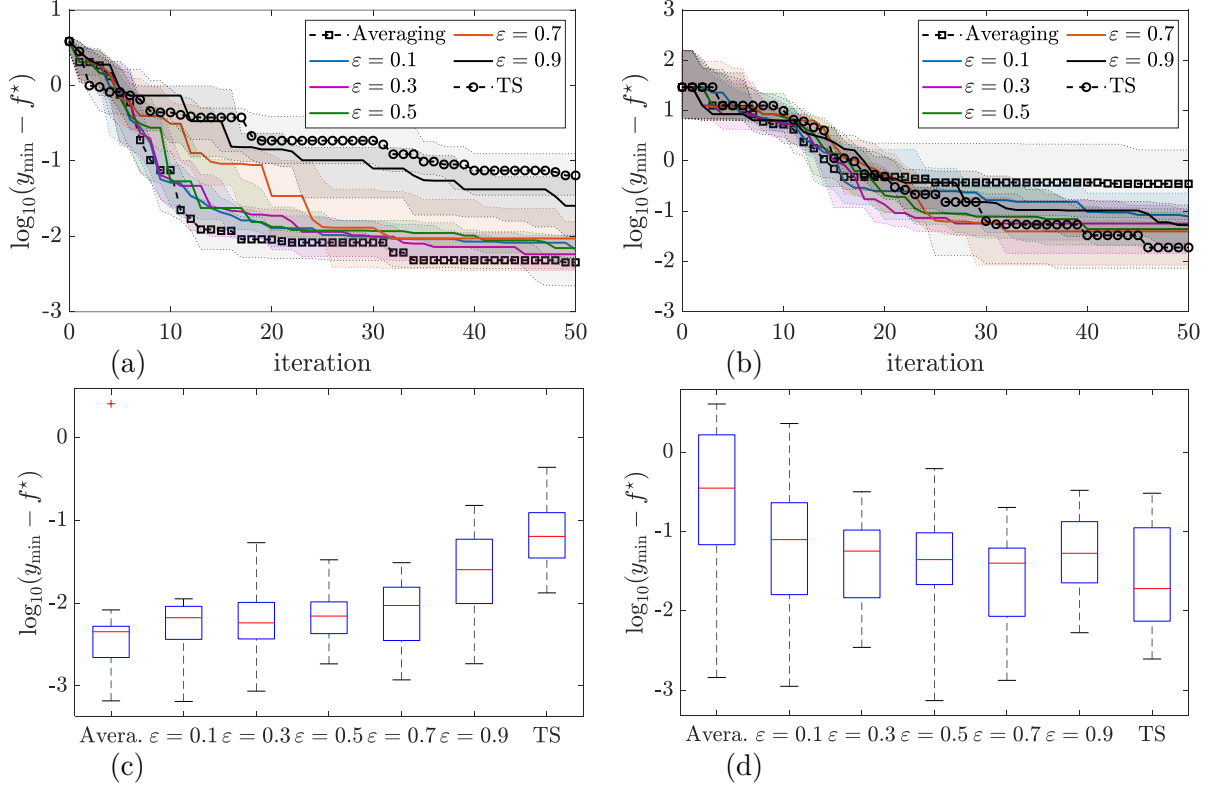


Figure 4: Performance ε -greedy TS for different ε values and $N_s = 50$. Medians and interquartile ranges from 15 runs of each method for (a) 2d Ackley function and (b) 2d Rosenbrock function; Medians, and the 25th and 75th percentiles from 15 best-found observations at iteration 50 for (c) 2d Ackley function and (d) 2d Rosenbrock function.

the 2d Ackley function) might be better addressed with a smaller ε . Unfortunately, it is unclear to determine whether a black-box objective function favors exploitation or exploration to locate its minimum. This, ironically, motivates the use of ε -greedy TS to prevent our search from wrong directions when prioritizing exploitation or exploration only. It is also worth noting that any attempts to find an optimal value of ε should correspond to a specific accuracy level of initial GP models because lowering the fidelity of GP models always encourages exploration, irrespective of the selection of ε .

4.4 Effect of sample path numbers

We investigate how N_s values affect the optimization results by setting $N_s \in \{20, 50, 100\}$ for fixed $\varepsilon = 0.5$. Figure 5 shows the medians, and the 25th and 75th percentiles of the best observations found at the last iteration for different N_s values. The solutions observed exhibit less sensitivity to changes in N_s when it reaches a sufficiently large value. This can be explained by an observation that increasing N_s while it is still sufficiently large has a modest impact on exploitation of ε -greedy TS; see Figures 10 and 11 of Appendix B.

4.5 Computational cost

We also investigate the effects of varying ε and N_s values on the runtime per dataset sample (i.e., unit runtime) for selecting the next input variable point. Figure 6 shows approximate distributions of unit runtime for selecting the next input variable point using the averaging TS with $N_s = 50$, ε -greedy TS with different ε values and $N_s = 50$, and the generic TS for the 2d Ackley and 2d Rosenbrock functions. Figure 7 shows similar quantities when ε -greedy TS uses different N_s values and fixed $\varepsilon = 0.5$. Here the generic TS corresponds to $N_s = 1$. We see in Figure 6 that increasing ε results in a slight decrease in the unit runtime. This observation can be attributed to the fact that a larger ε necessitates more exploration of calling the generic TS, which is generally cheaper than the averaging TS. In addition, the unit runtimes associated with $\varepsilon = 0.5$ and $\varepsilon = 0.9$ are comparable with that of the generic TS. Figure 7 shows marginal differences in empirical mode values of unit runtime for $N_s = 20$, $N_s = 50$, and the generic TS. An excessively large value of N_s , e.g., $N_s = 100$, increases the unit runtime of ε -greedy TS. However, it does not guarantee an improvement in the performance of ε -greedy TS; see Figure 5.

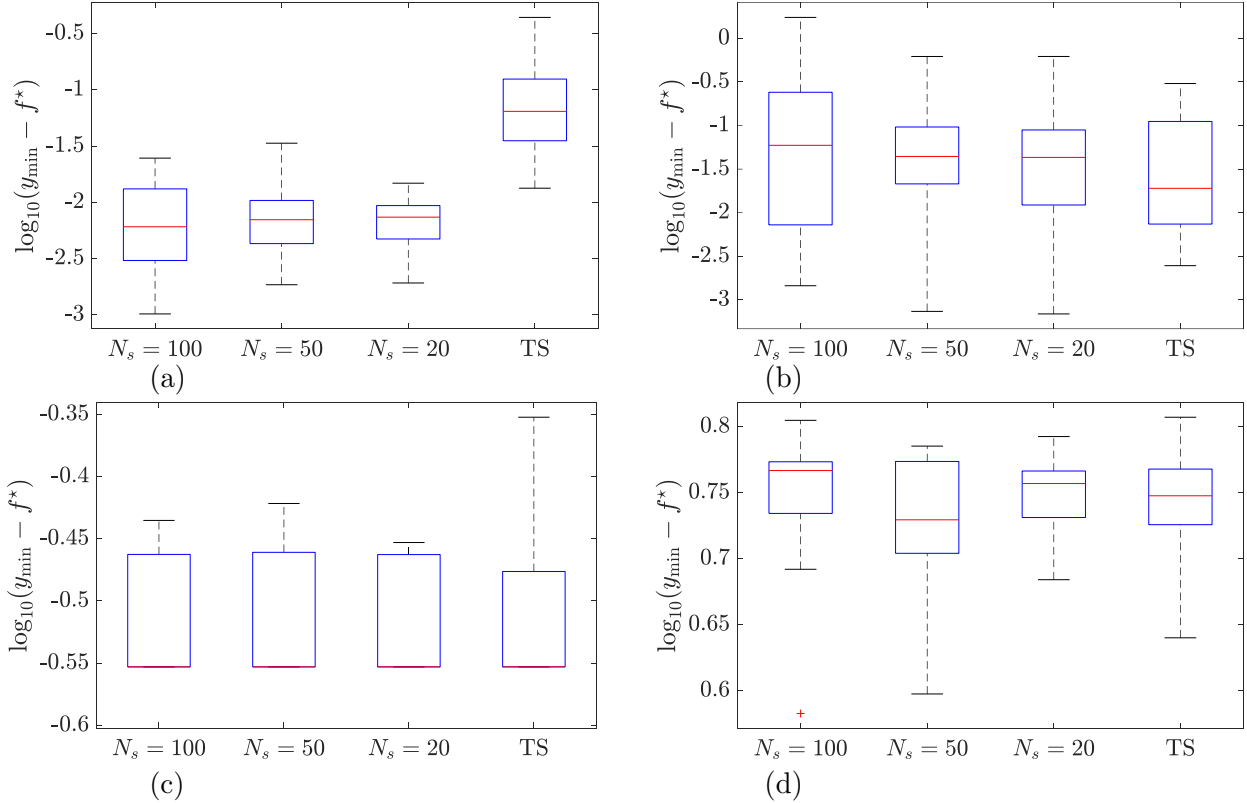


Figure 5: Performance ε -greedy TS for different N_s values and $\varepsilon = 0.5$. Medians, and the 25th and 75th percentiles from 15 best-found observations at the last iteration for (a) 2d Ackley function, (b) Rosenbrock function, (c) 6d Hartmann function, and (d) 10d Michalewicz function.

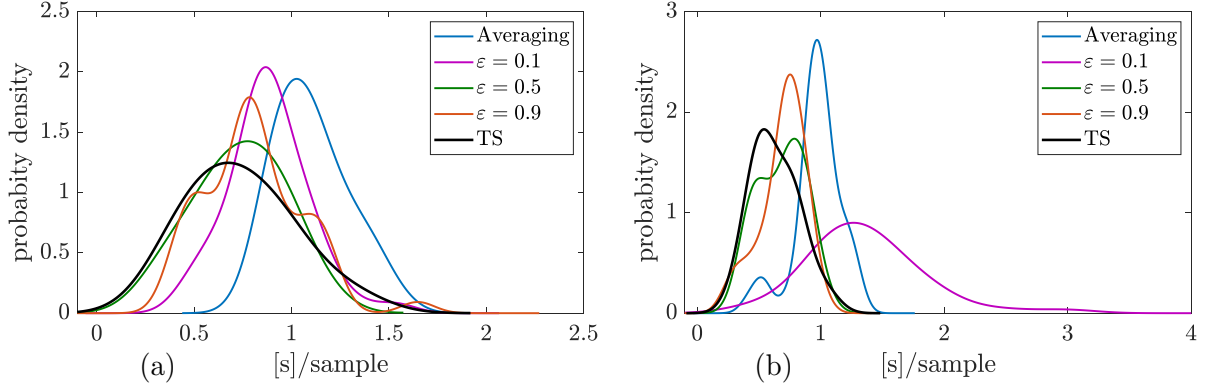


Figure 6: Approximate distributions of unit runtime for selecting the next input variable point with different ε values and $N_s = 50$. (a) 2d Ackley function; and (b) 2d Rosenbrock function.

5 Conclusion

We introduced ε -greedy TS to BO for optimizing costly objective functions. Our empirical findings reveal that the method for an appropriate value of ε outperforms one of its two extremes (i.e., the averaging TS and the generic TS) and competes with the other one. The computational cost of our method for a proper ε and a sufficiently large number of sample paths (e.g., $N_s = 20$ or 50) is comparable to that of the generic TS.

While several ε -greedy algorithms and the generic TS are guaranteed to converge eventually [3, 18], we look forward to a theoretical analysis to elucidate the convergence properties of ε -greedy TS. Additionally, we are keen on exploring

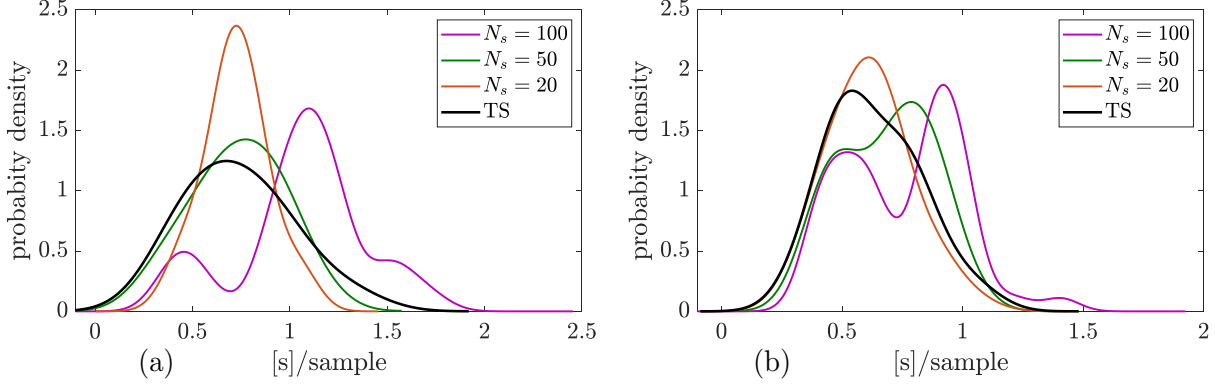


Figure 7: Approximate distributions of unit runtime for selecting the next input variable point with different N_s values and $\varepsilon = 0.5$. (a) 2d Ackley function; and (b) 2d Rosenbrock function.

its extensions to high-dimensional settings, e.g., with support from a subspace-based approach [30] or a trust-region method [31], and investigating its adaptability to varying ε during the optimization process.

References

- [1] Jasper Snoek, Hugo Larochelle, and Ryan P Adams. Practical Bayesian optimization of machine learning algorithms. In *Advances in Neural Information Processing Systems*, volume 25, pages 2951–2959. Curran Associates, Inc., 2012. URL https://proceedings.neurips.cc/paper_files/paper/2012/file/05311655a15b75fab86956663e1819cd-Paper.pdf. Cited on page 2.
- [2] Peter I. Frazier. Bayesian optimization. INFORMS TutORials in Operations Research, pages 255–278. INFORMS, October 2018. doi:10.1287/educ.2018.0188. URL <https://doi.org/10.1287/educ.2018.0188>. Cited on page 255.
- [3] Roman Garnett. *Bayesian optimization*. Cambridge University Press, Cambridge, 2023. ISBN 9781108425780. Cited on page 1.
- [4] Bach Do and Ruda Zhang. Multi-fidelity bayesian optimization in engineering design. arXiv, November 2023. URL <https://arxiv.org/abs/2311.13050>.
- [5] Philipp Hennig, Michael A. Osborne, and Hans P. Kersting. *Probabilistic numerics: Computation as machine learning*. Cambridge University Press, 2022. ISBN 1316730336. Cited on chapter 32.
- [6] Julien Villemonteix, Emmanuel Vazquez, and Eric Walter. An informational approach to the global optimization of expensive-to-evaluate functions. *Journal of Global Optimization*, 44(4):509–534, 2009. ISSN 1573-2916. doi:10.1007/s10898-008-9354-2. URL <https://doi.org/10.1007/s10898-008-9354-2>. Cited on pages 8, 9.
- [7] Philipp Hennig and Christian J. Schuler. Entropy search for information-efficient global optimization. *Journal of Machine Learning Research*, 13(6):1809–1837, 2012. ISSN 1532-4435. URL <https://www.jmlr.org/papers/v13/hennig12a.html>. Cited on page 2.
- [8] José Miguel Hernández-Lobato, Matthew W. Hoffman, and Zoubin Ghahramani. Predictive entropy search for efficient global optimization of black-box functions. In *Advances in Neural Information Processing Systems*, volume 27, pages 918–926. Curran Associates, Inc., 2014. URL https://proceedings.neurips.cc/paper_files/paper/2014/hash/069d3bb002acd8d7dd095917f9efe4cb-Abstract.html. Cited on page 3.
- [9] Zi Wang and Stefanie Jegelka. Max-value entropy search for efficient Bayesian optimization. In *Proceedings of the 34th International Conference on Machine Learning*, volume 70, pages 3627–3635. PMLR, 2017. URL <https://proceedings.mlr.press/v70/wang17e.html>. Cited on pages 2, 3, 4.
- [10] Donald R. Jones, Matthias Schonlau, and William J. Welch. Efficient global optimization of expensive black-box functions. *Journal of Global Optimization*, 13(4):455–492, 1998. ISSN 1573-2916. doi:10.1023/A:1008306431147. URL <https://doi.org/10.1023/A:1008306431147>. Cited on page 17.
- [11] András Sóbester, Stephen J. Leary, and Andy J. Keane. On the design of optimization strategies based on global response surface approximation models. *Journal of Global Optimization*, 33(1):31–59, 2005. ISSN 1573-2916. doi:10.1007/s10898-004-6733-1. URL <https://doi.org/10.1007/s10898-004-6733-1>. Cited on page 9.

- [12] Niranjan Srinivas, Andreas Krause, Sham M. Kakade, and Matthias Seeger. Gaussian process optimization in the bandit setting: No regret and experimental design. In *Proceedings of the 27th International Conference on International Conference on Machine Learning*, pages 1015–1022. Omnipress, 2010. URL <https://icml.cc/Conferences/2010/papers/422.pdf>. Cited on page 4.
- [13] Peter I. Frazier, Warren B. Powell, and Savas Dayanik. A knowledge-gradient policy for sequential information collection. *SIAM Journal on Control and Optimization*, 47(5):2410–2439, January 2008. ISSN 0363-0129. doi:10.1137/070693424. URL <https://doi.org/10.1137/070693424>. Cited on page 2.
- [14] Olivier Chapelle and Lihong Li. An empirical evaluation of Thompson sampling. In *Advances in Neural Information Processing Systems*, volume 24, pages 2249–2257. Curran Associates, Inc., 2011. URL https://papers.nips.cc/paper_files/paper/2011/hash/e53a0a2978c28872a4505bdb51db06dc-Abstract.html. Cited on page 2.
- [15] Daniel J. Russo, Benjamin Van Roy, Abbas Kazerouni, Ian Osband, and Zheng Wen. A tutorial on Thompson sampling. *Foundations and Trends® in Machine Learning*, 11(1):1–96, 2018. ISSN 1935-8237. doi:10.1561/2200000070. URL <http://dx.doi.org/10.1561/2200000070>. Cited on page 7.
- [16] Kirthevasan Kandasamy, Akshay Krishnamurthy, Jeff Schneider, and Barnabas Poczos. Parallelised bayesian optimisation via thompson sampling. In *Proceedings of the Twenty-First International Conference on Artificial Intelligence and Statistics*, volume 84 of *Proceedings of Machine Learning Research*, pages 133–142. PMLR, 09–11 Apr 2018. URL <https://proceedings.mlr.press/v84/kandasamy18a.html>. Cited on page 4.
- [17] Richard S Sutton and Andrew G Barto. *Reinforcement learning: An introduction*. MIT Press, 2018. ISBN 9780262039246. Cited on pages 28, 30, 32.
- [18] George De Ath, Richard M. Everson, Alma A. M. Rahat, and Jonathan E. Fieldsend. Greed Is Good: Exploration and Exploitation Trade-offs in Bayesian Optimisation. *ACM Transactions on Evolutionary Learning and Optimization*, 1(1), apr 2021. ISSN 2688-3007. doi:10.1145/3425501. URL <https://doi.org/10.1145/3425501>. Cited on pages 10, 11, 21.
- [19] Tianyuan Jin, Xianglin Yang, Xiaokui Xiao, and Pan Xu. Thompson sampling with less exploration is fast and optimal. In *Proceedings of the 40th International Conference on Machine Learning*, volume 202 of *Proceedings of Machine Learning Research*, pages 15239–15261. PMLR, 23–29 Jul 2023. URL <https://proceedings.mlr.press/v202/jin23b.html>. Cited on pages 3, 4.
- [20] Carl Edward Rasmussen and Christopher K I Williams. *Gaussian processes for machine learning*. The MIT Press, Massachusetts, USA, 2006. ISBN 9780521872508. doi:10.7551/mitpress/3206.001.0001. URL <https://doi.org/10.7551/mitpress/3206.001.0001>. Cited on page 2.
- [21] C. Bishop. *Pattern recognition and machine learning*. Springer, Berkeley, CA, USA, 2006. ISBN 9780387310732. Cited on page 87.
- [22] Holger Wendland. *Scattered data approximation*, volume 17. Cambridge University Press, 2004. ISBN 9780511264320. Cited on page 70.
- [23] Gabriel Riutort-Mayol, Paul-Christian Bürkner, Michael R. Andersen, Arno Solin, and Aki Vehtari. Practical Hilbert space approximate Bayesian Gaussian processes for probabilistic programming. *Statistics and Computing*, 33(1):17, 2022. ISSN 1573-1375. doi:10.1007/s11222-022-10167-2. URL <https://doi.org/10.1007/s11222-022-10167-2>. Cited on page 4.
- [24] Ali Rahimi and Benjamin Recht. Random features for large-scale kernel machines. In *Advances in Neural Information Processing Systems*, volume 20. Curran Associates, Inc., 2007. URL https://proceedings.neurips.cc/paper_files/paper/2007/file/013a006f03dbc5392effeb8f18fda755-Paper.pdf. Cited on page 1.
- [25] James T. Wilson, Viacheslav Borovitskiy, Alexander Terenin, Peter Mostowsky, and Marc Peter Deisenroth. Efficiently sampling functions from Gaussian process posteriors. In *Proceedings of the 37th International Conference on Machine Learning*, volume 119, pages 10292–10302. PMLR, 2020. URL <https://proceedings.mlr.press/v119/wilson20a.html>. Cited on pages 2, 3.
- [26] Maximilian Balandat, Brian Karrer, Daniel Jiang, Samuel Daulton, Ben Letham, Andrew G Wilson, and Eytan Bakshy. BoTorch: A Framework for Efficient Monte-Carlo Bayesian Optimization. In *Advances in Neural Information Processing Systems*, volume 33, pages 21524–21538. Curran Associates, Inc., 2020. URL https://proceedings.neurips.cc/paper_files/paper/2020/file/f5b1b89d98b7286673128a5fb112cb9a-Paper.pdf. Cited on pages 2, 3.
- [27] Eric Bradford, Artur M. Schweidtmann, and Alexei Lapkin. Efficient multiobjective optimization employing Gaussian processes, spectral sampling and a genetic algorithm. *Journal of Global Optimization*, 71(2):407–438, 2018. ISSN 1573-2916. doi:10.1007/s10898-018-0609-2. URL <https://doi.org/10.1007/s10898-018-0609-2>. Cited on page 14.

- [28] D. E. Finkel and C. T. Kelley. Additive scaling and the DIRECT algorithm. *Journal of Global Optimization*, 36(4):597–608, 2006. ISSN 1573-2916. doi:10.1007/s10898-006-9029-9. URL <https://doi.org/10.1007/s10898-006-9029-9>. Cited on pages 2, 3.
- [29] Alexander I. J. Forrester, András Sóbester, and Andy Keane. *Engineering design via surrogate modelling: A practical guide*. John Wiley & Sons, West Sussex, UK, 2008. ISBN 0470770791. Cited on page 15.
- [30] Amin Nayebi, Alexander Munteanu, and Matthias Poloczek. A framework for Bayesian optimization in embedded subspaces. In *Proceedings of the 36th International Conference on Machine Learning*, volume 97, pages 4752–4761. PMLR, 09–15 Jun 2019. URL <https://proceedings.mlr.press/v97/nayebi19a.html>. Cited on pages 2, 3.
- [31] David Eriksson, Michael Pearce, Jacob Gardner, Ryan D. Turner, and Matthias Poloczek. Scalable global optimization via local Bayesian optimization. In *Advances in Neural Information Processing Systems*, volume 32, pages 5496–5507. Curran Associates, Inc., 2019. URL https://proceedings.neurips.cc/paper_files/paper/2019/hash/6c990b7aca7bc7058f5e98ea909e924b-Abstract.html. Cited on pages 3, 4.
- [32] S Surjanovic and D Bingham. Virtual library of simulation experiments: Test functions and datasets, 2013. URL <http://www.sfu.ca/~ssurjano>.

A Benchmark test functions.

The analytical expressions for the test functions used in Section 4 are given below. The global solutions of these functions are detailed in [32].

Ackley function:

$$f(\mathbf{x}) = -a \exp \left(-b \sqrt{\frac{1}{d} \sum_{i=1}^d x_i^2} \right) - \exp \left(\frac{1}{d} \sum_{i=1}^d \cos(cx_i) \right) + a + \exp(1), \quad (11)$$

where d denotes the number of dimensions, $a = 20$, $b = 0.2$, and $c = 2\pi$. The function is evaluated on $\mathcal{X} = [-5, 5]^d$ and has a global minimum at $\mathbf{x}^* = \mathbf{0}$ with $f^* = f(\mathbf{x}^*) = 0$.

Rosenbrock function:

$$f(\mathbf{x}) = \sum_{i=1}^{d-1} [100(x_{i+1} - x_i^2)^2 + (x_i - 1)^2]. \quad (12)$$

The function is evaluated on $\mathcal{X} = [-5, 10]^d$ and has a global minimum at $\mathbf{x}^* = [1, \dots, 1]^\top$ with $f^* = f(\mathbf{x}^*) = 0$.

6d Hartmann function:

$$f(\mathbf{x}) = - \sum_{i=1}^4 a_i \exp \left(- \sum_{j=1}^6 A_{ij} (x_j - P_{ij})^2 \right), \quad (13)$$

where

$$\mathbf{a} = [1, 1.2, 3, 3.2]^\top, \quad (14a)$$

$$\mathbf{A} = \begin{bmatrix} 10 & 3 & 17 & 3.5 & 1.7 & 8 \\ 0.05 & 10 & 17 & 0.1 & 8 & 14 \\ 3 & 3.5 & 1.7 & 10 & 17 & 8 \\ 17 & 8 & 0.05 & 10 & 0.1 & 14 \end{bmatrix}, \quad (14b)$$

$$\mathbf{P} = 10^{-4} \begin{bmatrix} 1312 & 1696 & 5569 & 124 & 8283 & 5886 \\ 2329 & 4135 & 8307 & 3736 & 1004 & 9991 \\ 2348 & 1451 & 3522 & 2883 & 3047 & 6650 \\ 4047 & 8828 & 8732 & 5743 & 1091 & 381 \end{bmatrix}. \quad (14c)$$

The input domain of the function is $\mathcal{X} = [0, 1]^d$. The function has a global minimum at $\mathbf{x}^* = [0.20169, 0.150011, 0.476874, 0.275332, 0.311625, 0.6573]^\top$ with $f^* = f(\mathbf{x}^*) = -3.32237$.

Michalewicz function:

$$f(\mathbf{x}) = - \sum_{i=1}^d \sin(x_i) \sin^{2m} \left(\frac{ix_i^2}{\pi} \right), \quad (15)$$

where $m = 10$. The function is evaluated on $\mathcal{X} = [0, \pi]^d$ and has a global minimum value $f^* = -9.66015$ for $d = 10$.

B Additional results.

This section provides some additional results to show how ε and N_s values affect the exploration and exploitation of ε -greedy TS for the 2D Ackley and 2D Rosenbrock functions. Figures 8 and 9 show that increasing the value of ε significantly enhances the exploration of input variable space. The reduction in N_s exhibits a modest effect on exploration when it remains sufficiently large; see Figures 10 and 11.

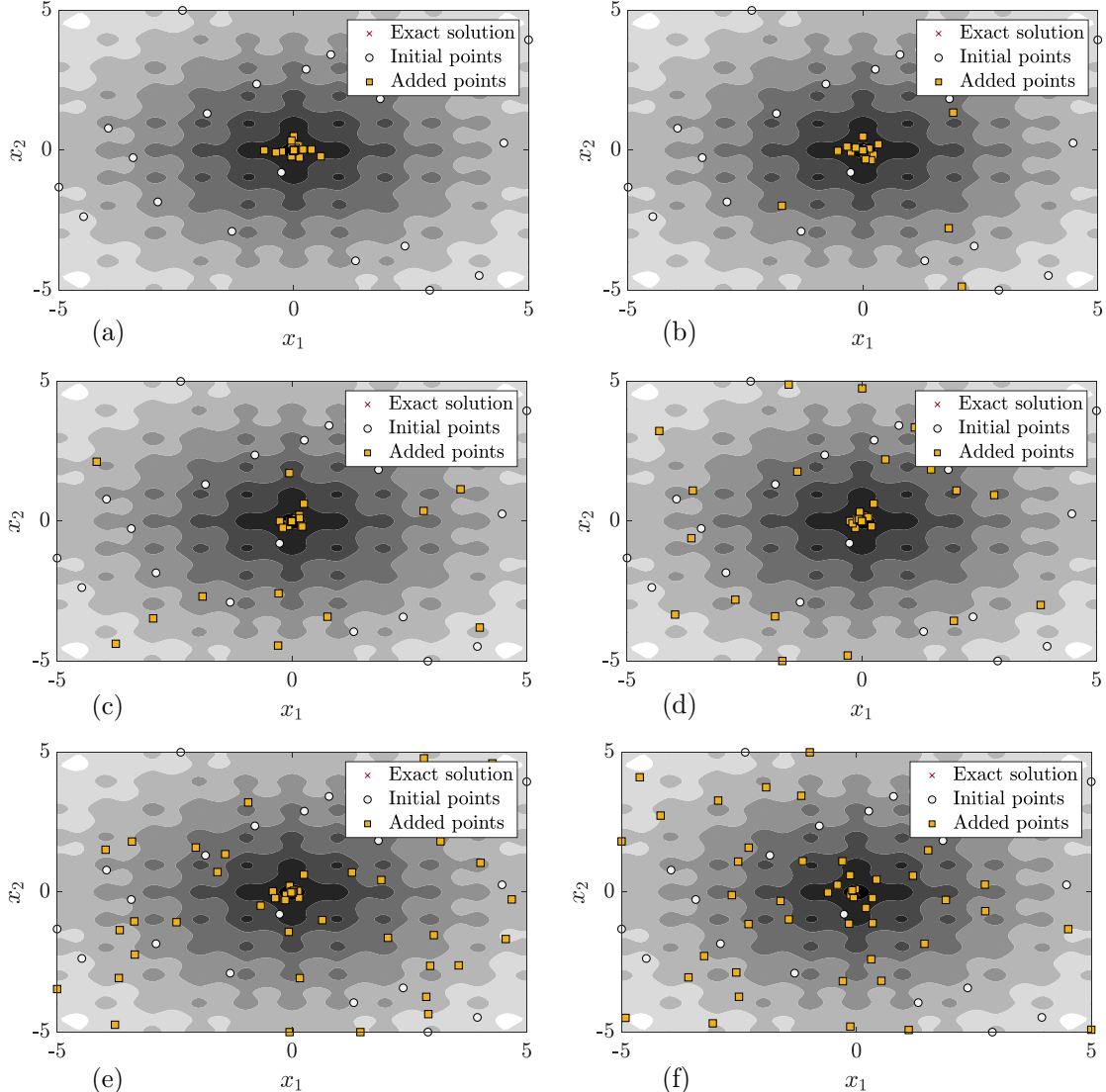


Figure 8: Initial and added points for 2D Ackley function with $N_s = 50$ and different values of ε . (a) Averaging ($\varepsilon = 0$); (b) $\varepsilon = 0.1$; (c) $\varepsilon = 0.3$; (d) $\varepsilon = 0.7$; (e) $\varepsilon = 0.9$; and (f) $\varepsilon = 1$ (TS).

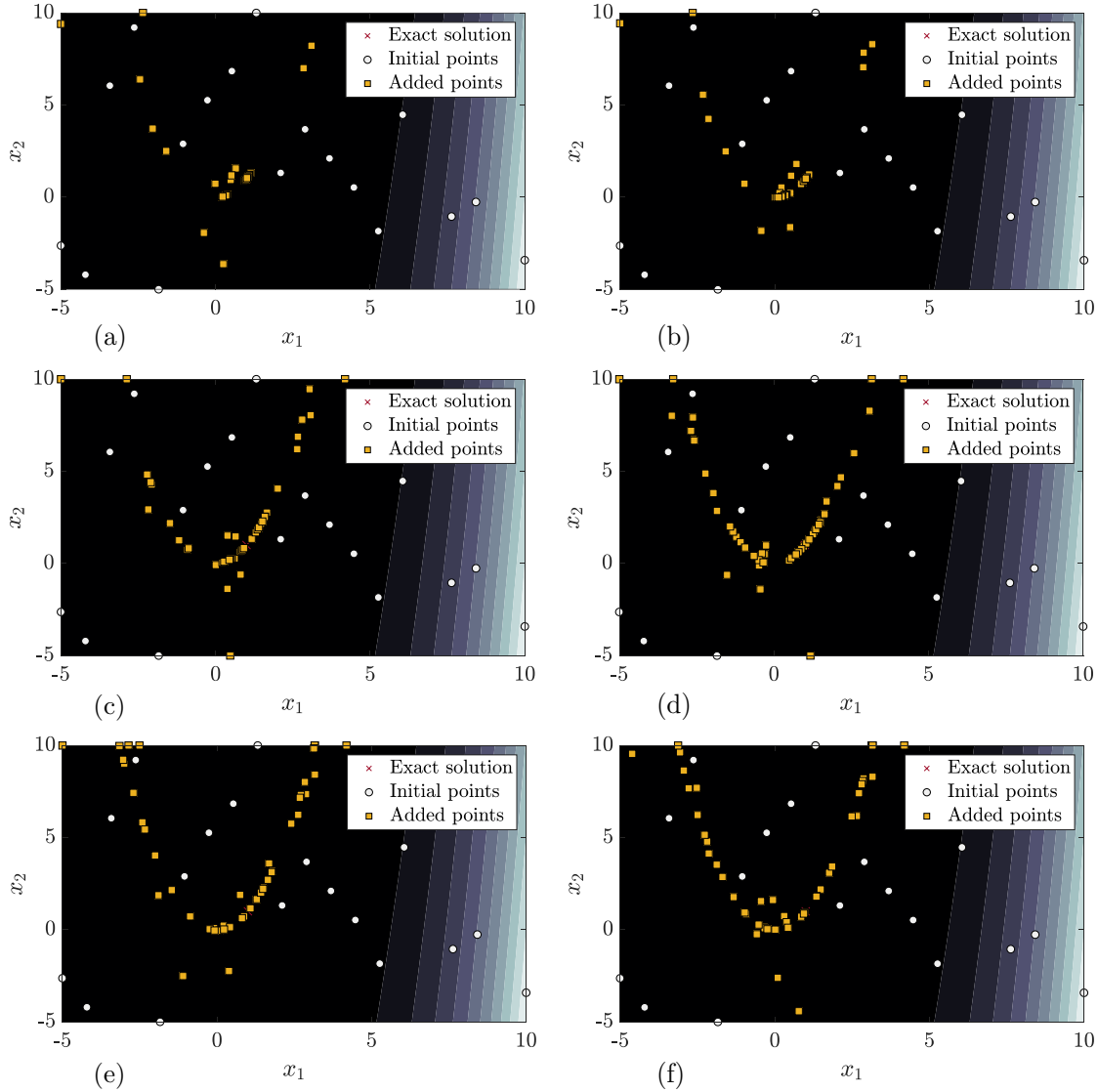


Figure 9: Initial and added points for 2D Rosenbrock function with $N_s = 50$ and different values of ε . (a) Averaging ($\varepsilon = 0$); (b) $\varepsilon = 0.1$; (c) $\varepsilon = 0.3$; (d) $\varepsilon = 0.7$; (e) $\varepsilon = 0.9$; and (f) $\varepsilon = 1$ (TS).

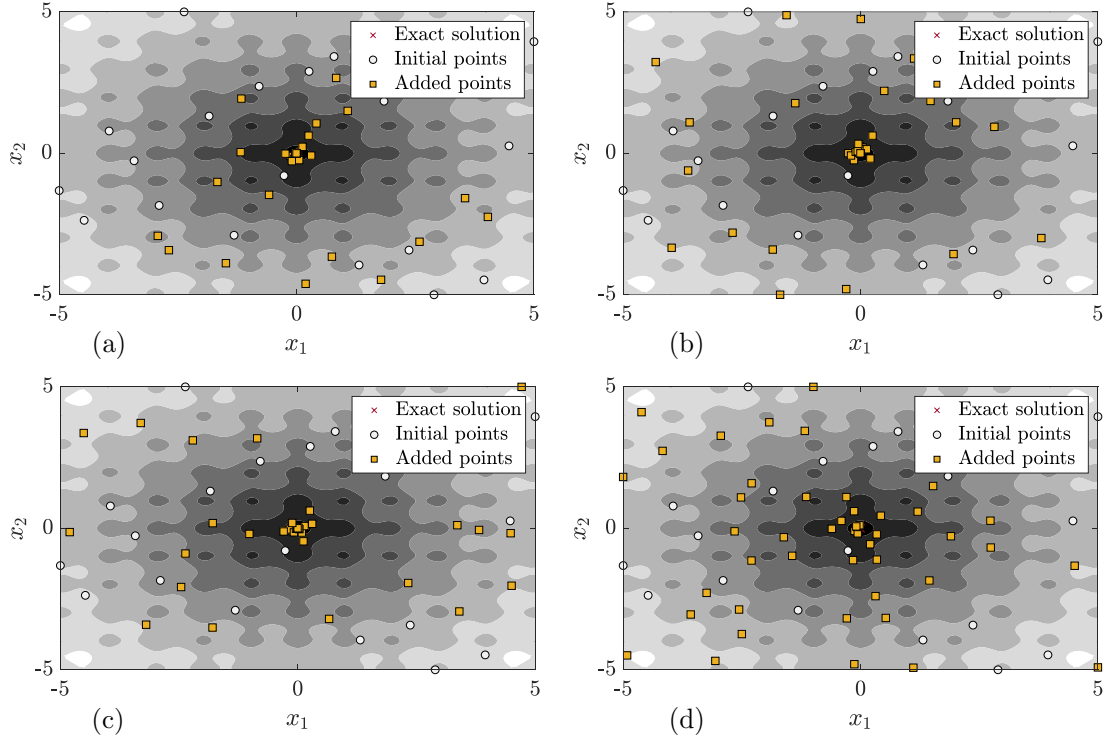


Figure 10: Initial and added input variable points for 2D Ackley function with $\varepsilon = 0.5$ and different values of N_s . (a) $N_s = 100$; (b) $N_s = 50$; (c) $N_s = 20$; and (d) $N_s = 1$ (TS).

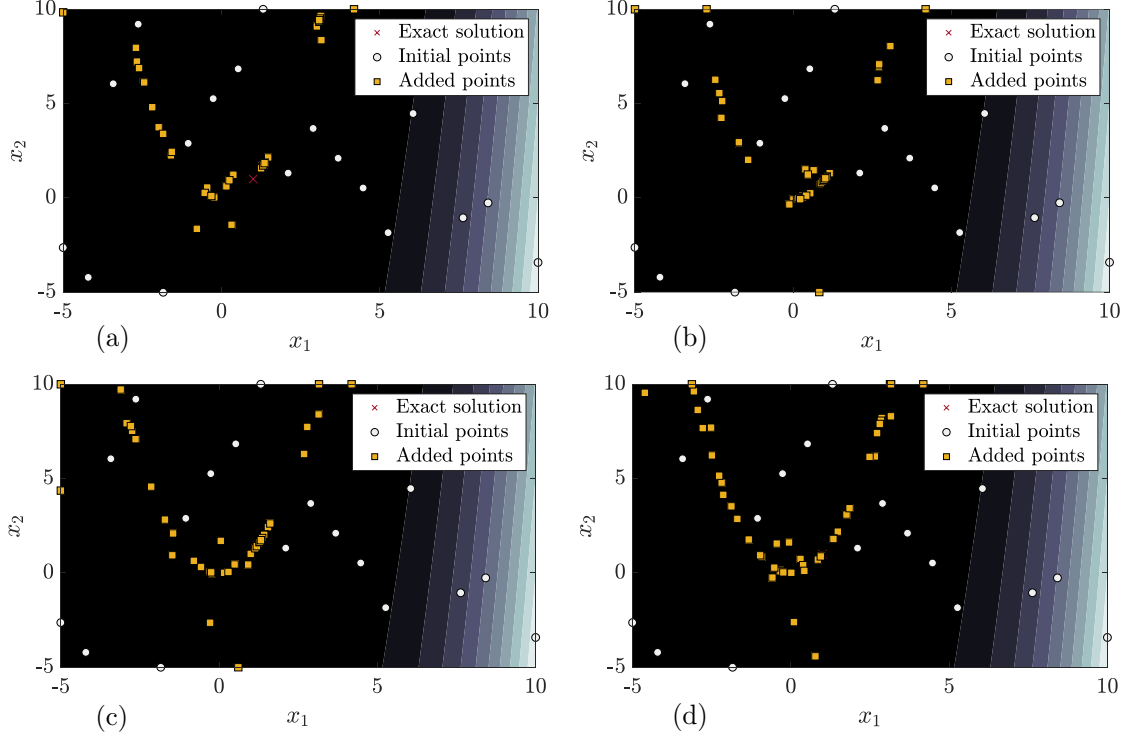


Figure 11: Initial and added input variable points for 2D Rosenbrock function with $\varepsilon = 0.5$ and different values of N_s . (a) $N_s = 100$; (b) $N_s = 50$; (c) $N_s = 20$; and (d) $N_s = 1$ (TS).